Journal of Radioanalytical and Nuclear Chemistry (2020) 324:409–421
https://doi.org/10.1007/s10967-020-07042-7

Uranium(VI) recovery from acidic leach liquor using manganese oxide coated zeolite (MOCZ) modified with amine

L. A. Yousef[1] · A. R. Bakry[1] · A. A. Ahmad[1]

Received: 20 December 2019 / Published online: 11 February 2020

Abstract
Manganese oxide coated zeolite modified with trioctyl amine (MOCZ/TOA) was tested for adsorption of uranium. Different experiments were performed to evaluate the optimum adsorption conditions; pH, dose, uranium concentration, temperature variation and contact time. Maximum adsorption capacity reached 99 mg/g according to Langmuir model. The study of thermodynamic parameters showed that sorption process is non spontaneous, exothermic and random. Studies on process kinetics showed that the process obeys pseudo-second order model. Uranium desorption was accomplished using 0.3 M H_2SO_4. Optimum conditions were carried out for uranium recovery from sedimentary geologic sample from Gattar area, North Eastern Desert, Egypt. The final uranium precipitate was characterized by ICP-OES technique.

Keywords MOCZ/TOA · Uranium(VI) · Kinetic · Equilibrium · Adsorption · Elution

Introduction

Several techniques are applied for radioactive metals uptake, including solvent extraction, ion exchange and direct precipitation [1–3]. Adsorption of the desired ions on the active surface of a solid matter followed by re-dissolution is a simple and economic technique, which is environmentally safe [4]. Many adsorbents are cost-effective because they are either naturally abundant or can be easily prepared [5].

Zeolites are highly effective at removing heavy metals from radioactive wastes and in soil remediation processes. After Fukushima nuclear disaster in Japan on 2011, zeolites were spread on agricultural soils in order to trap radioactive contaminants [6]. Zeolites are hydrated alumino-silicate minerals [$(Na_2, K_2, Ca, Ba)\ (Al,Si)O_2]_X{\cdot}nH_2O$ built up from interlinked alumina tetrahedra (AlO_4) and silica (SiO_4). There are about 40 naturally occurring zeolites found among both volcanic and sedimentary rocks; the most commonly mined forms include chabazite, clinoptilolite, and mordenite. Naturally occurring zeoliferous formations are significant materials for industrial and environmental applications [7–12].

Zeolites are widely used in domestic as well as commercial water treatment techniques. They act as ion-exchange water softeners; hard water (rich in calcium and magnesium) is piped through a column filled with sodium-zeolites which trap Mg^{2+} and Ca^{2+} ions while release Na^+ ions, rendering water softer [13, 14].

The crystal lattice of zeolites compromise tiny holes which are roughly of same size as small molecules. Such holes let small molecules pass through them while trap larger ones; that's why they're sometimes referred to as "molecular sieves". Such cage-like framework structure enables zeolites to perform as a cation exchange material [15]. The adsorptive properties of zeolites originate due to the presence of accessible hydroxyl groups associated with the tetrahedral framework. Alumina-rich zeolites are attracted to polar molecules such as water, while silica-rich zeolites work better with non-polar molecules [16].

Zeolite is available as a common conventional filter medium owing to its cheapness, safety and availability. However, further modification is needed to improve its adsorption capacity of heavy metal ions [17].

Manganese oxide is one of the most important scavengers of aqueous trace metal ions used for soil remediation due to its outstanding sorption behavior [18, 19]. Even in the presence of large concentrations of supporting electrolytes, weakly hydrolyzed cations are strongly adsorbed onto manganese oxide surfaces. Such surfaces possess large surface

✉ A. A. Ahmad
zarginah@gmail.com

[1] Nuclear Materials Authority, Cairo, Egypt

area, a microporous structure and high affinity for metal ions; providing an efficient scavenging pathway for heavy metal ions [20, 21].

However, coating manganese oxide onto a support surface may provide an effective means for the removal of heavy metal ions from aqueous solutions [22]. In order to improve the strength of pure manganese oxide and to enhance its capability of removing heavy metal ions, a modified method of coating the surface of zeolite with manganese oxide integrated with trioctylamine has been developed. A method of coating zeolite with a thin layer of manganese oxide enhances its sorption capacity towards metal ions relative to uncoated zeolite. The enhanced capacity towards uranium uptake is a result of the amphoteric surface charge provided by coating with manganese oxide. Such method provides an effective surface for radioactive metal adsorption [23].

Gabal Gattar is a promising area with wide distribution of uranium occurrences. The occurrence of interest is hosted in El Hammamat sediments that occur at the northwestern area of Gattar granite pluton. Uraniferous mineralizations of Gabal Gattar are located 35 km west of Hurghada, Egypt. The mineralization can be considered as a uranium ore material associated with other valuable minerals [24]. Uranium mineralizations are represented by Precambrian Calc-Alkaline granites (Late Orogenic Plutonites). Uranium mineralizations are mainly located at the shear structures cutting across granitic masses and are associated with quartz veinlets. The studied sample was hosted within younger granite. Such granites exhibit extensive alteration, including Na– and K– metasomatism, silicification, argillization, chloritization, and pyritization [25].

A magnetic polystyrene (PS) trioctylamine (Fe_3O_4/PS/TOA) adsorbent was synthesized on a porous polystyrene microsphere matrix with a crosslinking degree of 0.5% and applied for removal of simulated radioactive element Ce^{3+} [26]. Montmorillonite (Mt) was used to remove copper (Cu^{2+}) ion from wastewater stream generated from industrial effluents. This clay was modified (Mt-TOA) by using (TOA) [27].

The removal of erythrosine by magnetic iron oxide nanoparticles modified by methyl trioctyl ammonium chloride has been previously studied. FTIR and TEM were applied for characterization of the modified iron oxide nanoparticles [28]. This study focused on stability issues facing amine-functionalized adsorbents, including amine-grafted and amine-impregnated silicas, zeolites, metal–organic frameworks and carbons.

Recently, major advances were achieved in understanding and improving the performance of such materials in terms of adsorption capacity, selectivity and adsorption kinetics [29]. Introducing amine groups to the surface of an adsorbent enhances its affinity to different organic and inorganic contaminants [30]. Different silica aerogels and crygels were modified with amine groups [31–34]. Other research groups also modified silica aerogels with thiol and amine groups [35, 36]. Such materials featured enhanced adsorption properties when compared to activated carbon, biochar or natural zeolites [37], achieving adsorption capacities one order of magnitude greater in the best scenarios.

The purpose of the present study was to test the properties of manganese oxide-coated zeolite (MOCZ) modified with trioctylamine (TOA) as an adsorbent for removing U(VI) ions from acidic solutions. For this purpose, the (MOCZ) modified with amine was synthesized and characterized. The effects of several variables, such as the initial U(VI) ion concentration, adsorbent dose, contact time, pH and temperature were investigated.

Experimental

Reagents

All the chemicals and reagents used are analytical grade. Uranium stock solution (1000 mg/L) was prepared by UO_2SO_4 crystals. U(VI) was estimated by oxidimetric titration using NH_4VO_3 [38]. Results were confirmed spectrometrically by Arsenazo III at $\lambda = 655$ nm [39].

Instrumentation

The absorbance of uranium, SiO_2, Al_2O_3, TiO_2, and P_2O_5 was measured using Metertech Inc, model SP-8001, UV–visible spectrophotometer. Na^+ and K^+ were determined by a Sherwood flame photometer model 410 (England). CaO, MgO and total iron content were determined volumetrically [40]. Trace elements were detected using ICP-OES [41].

FTIR (Thermo Scientific—NICOLET IS10 USA) spectrometer was used to characterize functional groups of modified MOCZ before and after uranium adsorption. Scanning electron microscope (SEM) was used illustrate the surface morphology of the modified MOCZ.

Synthesis of modified MOCZ

MOCZ was synthesized according to Runping et al. (2007) and Weihua et al. (2009) [42, 43] with slight modification. A sample of Yemeni zeolite from "Alix zeolite Co". was ground to − 12 mesh size and immersed in water overnight to decrease its alkalinity. Colloidal MnO was precipitated on zeolite surface by reductive procedure. Hot $KMnO_4$ (0.5 M) solution was added to the dried zeolite. Hydrochloric acid (37.5%) was added drop wise to the mixture and agitated for 1 h. The product was filtered, washed to pH 7.0 with distilled water and dried.

Prepared MOCZ was modified by mixing 1:2 of MOCZ and hexamine ($C_6H_{12}N_4$). The mixture was added to 150 ml of distilled water and stirred for 2 h. The dried powder was stirred with 5% of tri-ethanol amine dissolved in ethanol for 1 h then filtered and dried out. Different concentrations (0.005–0.035 M) of tri-octyl amine TOA in benzene with S/L ratio (1/5) were used to modify the mixture. The modified (MOCZ/ amine) was filtered and dried overnight. The chemical analysis of natural zeolite is shown in (Table 1).

Hammamat sedimentary sample

The studied rock sample was collected from Gattar area, NE Desert, Egypt. It was ground into powder then attacked by a mixture of acids HF, HNO_3, $HClO_4$ and HCl in order to determine the chemical composition of major oxides and trace elements (mg/kg); (Table 2).

The preparation of studied leach liquor

The studied rock sample was ground and subjected to uranium leaching using the most favorable leaching conditions; − 200 mesh size, 5 M H_2SO_4, 1/4 solid/liquid ratio, 200 rpm stirring speed for 0.5 h. at room temperature. The solution was filtered and uranium was measured in the leach liquor. Uranium assayed 510 mg/L in the resulting leach liquor. The estimated uranium leaching efficiency was 85%.

Adsorption procedures

All adsorption studies are conducted by stirring of the solution containing uranium with a suitable amount of composite for a certain time under controlled temperature till equilibrium is achieved. To determine the optimum parameters, the pH was varied ranging from 1 to 12 and initial uranium concentration was varied from 50 to 800 mg/L at different contact times ranging from 5 to 40 min at different temperatures and composite doses.

After each experiment, the modified zeolite was filtered off and uranium was measured in the filtrate. The uranium uptake capacity (q_e, mg/g), adsorption efficiency (E%) and distribution coefficient (K_d) were calculated from the following equations:

$$q_e = (C_o - C_e) \times \left[\frac{v}{m}\right] \quad (1)$$

$$E(\%) = 100\left(C_o - C_e\right)/C_o \quad (2)$$

$$K_d = \frac{C_o - C_e}{C_o} \times \left[\frac{v}{m}\right] \quad (3)$$

where C_o and C_e stand for the initial uranium concentration and that at equilibrium (mg/L), respectively. V is the volume of aqueous solution (L) and m is the dry composite weight (g).

Results and discussions

The influence of pH

The abundance of hydrogen ions in solution plays an important role in the overall process of uranium adsorption in general, where pH has a direct influence on the aqueous chemistry of uranium as well as the properties of the active sites on the surface of the sorbent [44]. The adsorption of uranium by the modified MOCZ was studied in pH range 1–12 using 20 mL of solution assaying 500 mg/L of uranium, 0.1 g of adsorbent and 200 rpm stirring speed for 20 min at room

Table 1 Composition of major oxides (wt%) and trace elements (mg/kg) of natural zeolite

Major oxide	SiO_2	Al_2O_3	$Fe_2O_3^T$	CaO	MgO	P_2O_5	Na_2O	K_2O	MnO	TiO_2	SO_3	L.O.I
(wt%)	62.09	12.61	1.911	3.643	1.578	0.056	0.691	3.488	0.071	0.102	0.303	13.453
Trace element	Cr	Ni	Cu	Zn	Ga	As	Rb	Sr	Zr	Nb	Ba	Pb
(mg/kg)	52	137	135	46	21	140	277	825	68	10	454	58

Table 2 Composition of major oxides and trace elements by ICP-OES of sedimentary sample

Major oxide	SiO_2	Al_2O_3	$Fe_2O_3^T$	CaO	MgO	P_2O_5	Na_2O	MnO	TiO_2	L.O.I
Wt,%	72.31	12.46	3.61	1.56	1.83	0.31	3.60	0.07	0.58	1.20
Trace element	Cr	Ni	Cu	Zn	Co	Y	Hf	Zr	Nb	Ba	Pb	U
(mg/kg)	50	44	30	510	9	700	9	190	160	360	400	2400

temperature. It was observed that uranium adsorption efficiency increased on increasing pH from 1 to 4 till reaching a maximum at pH 4 (adsorption efficiency = 94.5%). Further increase in pH is accompanied by a decrease in adsorption efficiency (Fig. 1). Such behavior can be explained by the existence of 3 adsorption stages. The first stage is at pH < 3, showing low sorption capacity, which is attributed to the protonation of sorbent surface, causing an electrostatic repulsive forces with neighboring uranium ions [45, 46]. The second stage at pH 3–4, involving the increase of Adsorptivity with increasing the pH till reaching maximum sorption capacity at pH = 4, which is due to the decrease in + ve competition onto the sorbent, favoring U^{+6} ions adsorption. The third stage is at pH > 4, showing gradual decrease of uranium adsorption, due to the domination of the negatively charged uranium species within the bulk solution.

The influence of contact time

The effect of contact time was studied in a range of 5–40 min while other parameters were kept constant. The adsorption efficiency increased from 48% at 5 min to 94.5% at 20 min (Fig. 2). Furthermore, no significant increase in uranium adsorption took place, revealing that equilibrium state has been reached. This is an indication that monolayer coverage on the outer interface of the adsorbent took place [47]. When all the sites present on adsorbent became occupied, there was no increase in the percent of metal ions uptake [48]. On the other hand, a decrease in the uptake percent with increasing time may be encountered, due to internal particle diffusion processes dominating over adsorption [49].

The influence of initial uranium concentration

A series of 20 ml solutions of different initial uranium concentrations ranging from 50 to 800 mg/L were mixed each with 0.1 g of adsorbent at pH 4 and 200 rpm stirring speed for 20 min. The effect of initial uranium concentration was expressed in terms of both adsorption efficiency and maximum uptake (q_e), (Fig. 3). Results showed that uranium adsorption efficiency decreased from 95.5 to 94.5% with increasing uranium content from 50 to 500 mg/L, and dramatically decreased to 58.8% at 800 mg/L initial uranium concentration. Accordingly, 500 mg/L of uranium was found the most suitable concentration for the adsorption process. The limited number of active sites present on the adsorbent surface limits the capacity of the adsorbent to a certain uranium concentration [50]. On increasing the uranium concentration, uranium molecules will compete for the available

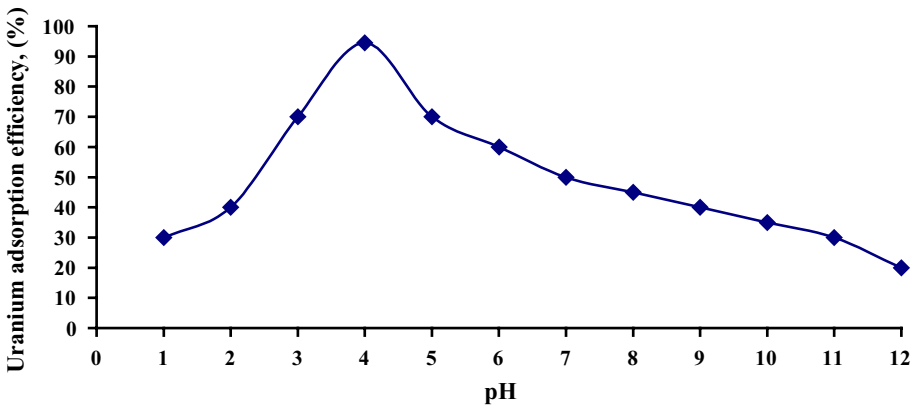

Fig. 1 Effect of pH on uranium adsorption efficiency using MOCZ modified with amine. *Adsorption conditions* 500 ppm uranium concentration, 20 min contact time, room temperature, 20 mL of uranium solution and 0.1 g modified (MOCZ) with amine

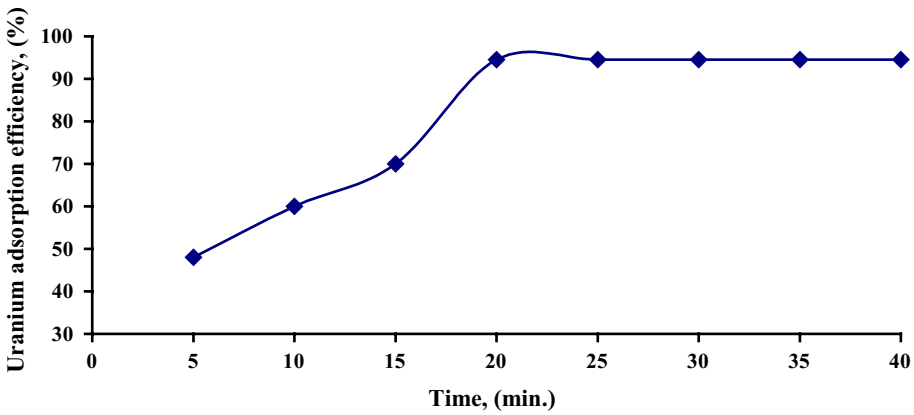

Fig. 2 Effect of contact time on uranium adsorption efficiency using MOCZ modified with amine. *Adsorption conditions* 500 ppm uranium concentration, pH: 4, room temperature, 20 mL of uranium solution and 0.1 g MOCZ modified with amine

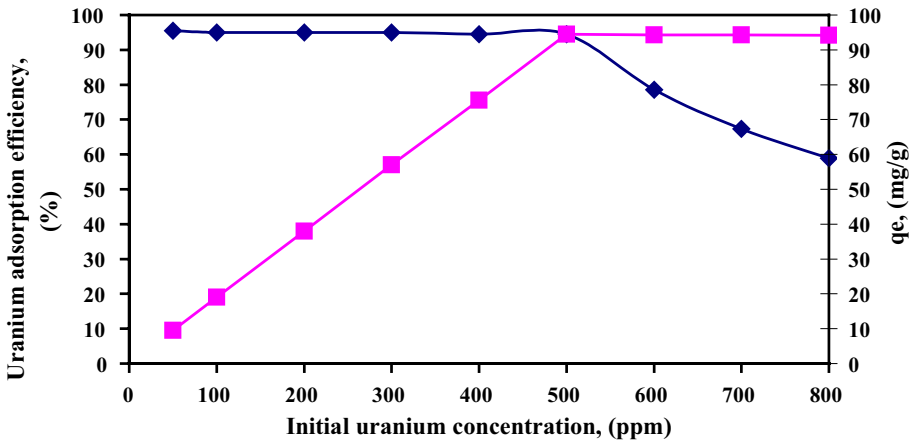

Fig. 3 Effect of initial uranium concentration on adsorption efficiency using MOCZ modified with amine. *Adsorption conditions* pH:4, 20 min contact time, room temperature, 20 mL of uranium solution and 0.1 g MOCZ modified with amine

functional groups on the surface of the adsorbent, leading to a decrease in the overall adsorption percent [51].

Influence of temperature

This factor was studied by performing several experiments at different temperatures ranging from 25 to 80 °C while keeping other parameters constant; 500 mg/L initial uranium concentration, pH 4 and 200 rpm agitation speed for 20 min.

The observed uranium adsorption efficiency decreased from 94.5% at 25 °C to 40% at 80 °C (Fig. 4). Consequently, room temperature was chosen as the most suitable temperature for uranium adsorption by the studied adsorbent (adsorption efficiency = 94.5%).

This happens owing to the physical nature of adsorption process as well as the nature of the chelating TOA group within the matrix, where bond cleavage between TOA and uranium may be encountered at elevated temperatures [52]. Previous work on the adsorption efficiency of acid cured phosphate rock towards uranyl ions from aqueous solution indicated better adsorption efficiencies at low temperatures [53, 54]. However, the negative effect of temperature on adsorption process indicates an exothermic nature [55, 56].

The influence of (V/m) ratio

The effect of (V/m) ratio has been investigated ranged from 0.1 to 1 at optimum conditions of other factors. It was found that, the uranium adsorption efficiency increases from 30% with (0.1 ratio) till 94.5% with (0.2 ratio) then the adsorption efficiency decreases with increasing (V/m) ratio, (Fig. 5). Therefore, the required (V/m) ratio to adsorb uranium ion was chosen 0.2 of ratio. In the first part of the curve, the increase in efficiency is attributed to an increase in the active surface available for the adsorbed material. Although, increasing the adsorbent dose leads to increasing the removed amount, but the amount of adsorbate per unit mass of adsorbent (uptake efficiency) gradually decreases due to the excessive amount of the sorbent available for adsorption. In other words; the amount of sorbent becomes more than enough compared to the amount of uranium inside solution. Therefore, at equilibrium, the amount of uranium present in solution will be distributed on a large amount of adsorbent, and the calculated adsorbent capacity in this case shall be lower than expected [57–59].

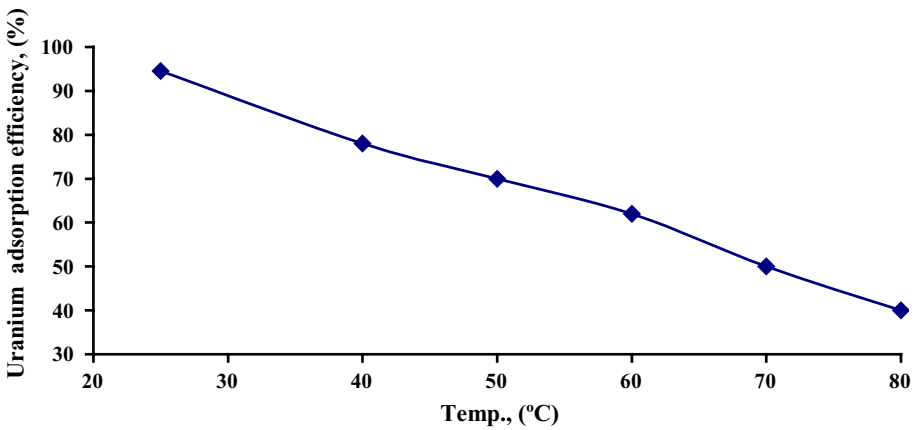

Fig. 4 Effect of temperature on uranium adsorption using MOCZ modified with amine. *Adsorption conditions* 500 ppm uranium concentration, 20 min contact time, pH: 4, 20 mL of uranium solution and 0.1 g MOCZ modified with amine

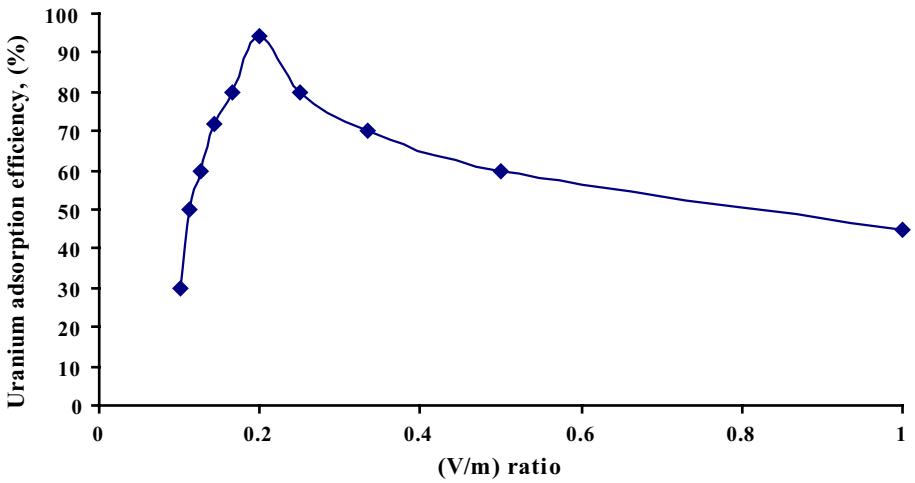

Fig. 5 Effect of (V/m) ratio on uranium adsorption using MOCZ modified with amine. *Adsorption conditions* 500 ppm uranium concentration, 20 min contact time, room temperature and pH: 4

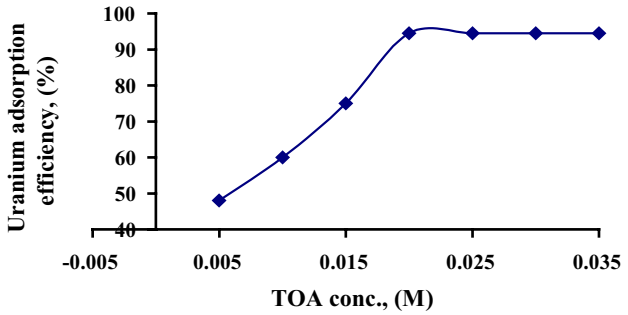

Fig. 6 Effect of TOA concentration on uranium adsorption efficiency using MOCZ. *Adsorption conditions* 500 ppm uranium concentration pH:4, 20 min contact time, room temperature, 20 mL of uranium solution

The influence of tri-octyl amine (TOA) concentration

The effect of TOA concentration impregnated upon 0.1 g of mixture of MOCZ, hexamine and tri-ethanol amine on uranium adsorption efficiency was studied. Different concentrations of TOA in benzene ranging from 0.005 to 0.035 M were stirred with MOCZ-amine, S/L ratio (1/5) for 20 min at room temperature (Fig. 6). Results show that uranium adsorption efficiency increase with increasing of the concentration of the (TOA) until reaching a maximum at 0.02 M TOA.

Uranium desorption from the modified MOCZ

Desorption is an important economic parameter in studying adsorption processes [60]. Three mineral acids (H_2SO_4, HCl and HNO_3) were tested for such purpose. A solution of 10 mL in volume and variable acid concentration ranging from 0.1 to 1 M was allowed each time to elute 0.1 g of loaded adsorbent for 20 min. The obtained results show that uranium elution efficiency increased by increasing acid concentration, where it reached 95% with 10 mL of 0.3 M H_2SO_4 from 0.1 g loaded adsorbent.

During the elution process, the unused portion of sulphuric acid is retained on the barren adsorbent, and then it is returned back into the absorption system, recycling it back into the leaching process, leading to an overall decrease of acid consumption. Sulphuric acid is preferred for elution procedures than HCl and HNO_3 due to higher elution efficiency, availability, excellent physical stability, and higher regeneration efficiency [61].

Adsorption equilibrium studies

Studying different adsorption isotherms of a certain process can help to figure out the most possible mechanism of the overall adsorption process. Uranium ions can be adsorbed onto the surface of the adsorbent by several possible mechanisms. The adsorption mechanism may depend on the nature of sorption sites, surface properties, affinity of the sorbent, the chemistry of the sorbate and the bulk properties of the aqueous solution [62, 63].

To investigate the best fitting isotherm model, sorption experiments were carried out at the most favorable adsorption conditions. 20 ml of pH 4 solution containing 500 mg/L initial uranium concentration was contacted with 0.1 g of the modified MOCZ at 200 rpm stirring speed for 20 min at room temp.

The most frequently used sorption models for adsorption studies are Langmuir and Freundlich. Both models were used to correlate experimental data at room temperature.

The Langmuir model assumes that maximum adsorption occurs as a saturated monolayer of adsorbate molecules on the adsorbent surface which is not accompanied by any transmigration of adsorbate molecules on the surface and that the energy of the adsorption process is constant [64]. It can be represented by the following equation:

$$\frac{C_e}{q_e} = \frac{1}{bq_{max}} + \frac{C_e}{q_{max}} \quad (4)$$

where C_e is the concentration of uranium in the solution at equilibrium (mg/L), q_e is the amount of uranium adsorbed per weight unit of the adsorbent at equilibrium (mg/g), q_{max} is the saturated monolayer adsorption capacity (mg/g) and b is the Langmuir constant (L/mg). The linear plots of Ce/qe versus Ce are shown in (Fig. 7). Table 3 clarifies that the calculated values of q_{max} are very close to experimental values with correlation coefficient $R^2 = 0.9967$. Results thus indicate that uranium adsorption process by the studied modified MOCZ obeys Langmuir isotherm model. The surface of the synthesized modified MOCZ is homogeneous and all metal binding sites are energetically the same. The adsorption process is monolayer in nature, and there are neither interactions between adsorbed molecules nor transmigration of sorbate molecules on the surface of adsorbent [65].

To predict whether a sorption system is favorable or unfavorable, the separation factor R_L was evaluated from the following equation [66]:

$$R_L = \frac{1}{1 + bC_o} \quad (5)$$

where b is the Langmuir constant and C_o (mg/L) is the initial U(VI) concentration. The value of R_L indicates the nature of the adsorption process; if $R_L = 0$ then the process is irreversible, if $(0 < R_L < 1)$ then the process is said to be favorable and if $(R_L = 1)$ the isotherm shall be linear and if $(R_L > 1)$ then the overall process is unfavorable. The obtained data clearly shows that in all cases $0 < R_L < 1$, indicating thereby a favorable sorption process for the studied metal ions under the conditions used in this study.

The Freundlich isotherm model assumes that adsorption occurs on a heterogeneous surface with a heterogeneous energetic distribution of active sites, accompanied by interactions between adsorbed molecules [67].

Table 3 Adsorption isotherm parameters for uranium adsorption by MOCZ/amine

Adsorption isotherm	Parameters	298 K
Langmuir isotherm	Equation	Y = 0.0101x + 0.1249
	q max (mg/g)	99
	b (L/mg)	0.080
	R^2	0.9967
Freundlich isotherm	Equation	Y = 0.4167x + 1.1022
	k_f (mg/g)	12.563
	1/n (mg min/g)	0.4167
	R^2	0.7357

The Freundlich isotherm model is represented by the following equation:

$$\mathrm{Log}q_e = \mathrm{Log}K_f + \left(\frac{1}{n}\right)\mathrm{Log}C_e \quad (6)$$

where q_e is the amount of uranium(VI) adsorbed at equilibrium (mg/g), C_e is the aqueous concentration of uranium at equilibrium, K_f is the adsorption capacity (mg/g) and n is the favorability constant related to the energy of adsorption. The Freundlich constants; K_f and 1/n are calculated from the slope and intercept of the log q_e versus log C_e plots. The adsorption parameters are shown in (Table 3). The values of K_f (mg/g) are lower than the experimental values of uranium adsorption by the modified MOCZ at room temperature. The obtained data shows that the modified MOCZ do not possess an energetically heterogeneous surface and the Freundlich isotherm does not fit with the obtained experimental data.

Sorption kinetics studies

The study of kinetic parameters is helpful in prediction of adsorption rate and supplies important information for modeling and design of extraction processes. Two kinetic models including pseudo-first order and pseudo-second

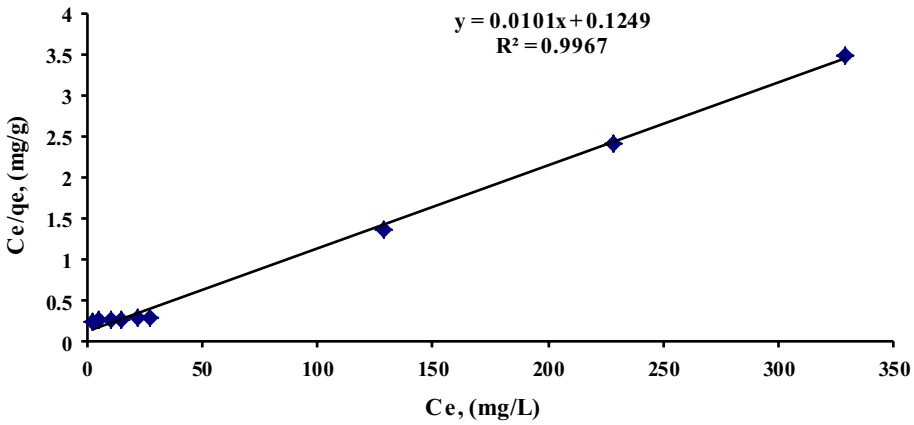

Fig. 7 Langmuir isotherm model of U(VI) adsorption by MOCZ modified with amine

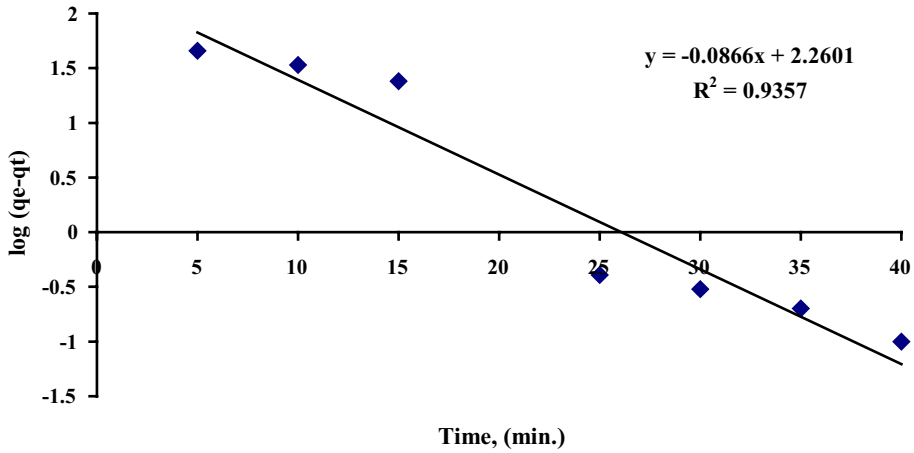

Fig. 8 Pseudo first order model of U(VI) onto the (MOCZ) modified with amine

Table 4 Kinetic model parameters applied to uranium onto MOCZ modified with amine

Kinetic models	Parameters	298 K
First order parameter	q_e (mg/g)	182
	K_1 (min^{-1})	0.199
	R^2	0.9357
Second order parameter	q_e (mg/g)	116.27
	K_2 (g/mg min)	0.00113
	R^2	0.9777

order diffusion models were applied to analyze the sorption kinetic process. The kinetics of uranium adsorption by the modified MOCZ was studied at 500 mg/L, constant pH 4, 200 rpm stirring speed at room temperature.

The following equation represents the linear form of pseudo-first order model [68]:

$$\mathrm{Log}(q_e - q_t) = \mathrm{Log}q_e - \left(\frac{K_1}{2.303}\right)t \quad (7)$$

where q_t and q_e are the amounts of uranium ions adsorbed at time t (min) and at equilibrium respectively, while k_1 is the adsorption rate constant (1/min). It can be determined by plotting Log ($q_e - q_t$) versus t (Fig. 8). The sorption capacity is determined from the intercept of the plots and was found to be 182 mg/g. The R^2 value equals 0.9357 at 500 mg/L initial uranium concentration. The adsorption process thus do not fit with pseudo-first order kinetic model (Table 4).

Experimental data were applied to pseudo-second order kinetic model in the form [69]:

$$\frac{t}{q_t} = \frac{1}{k_2 q_e^2} + \left(\frac{1}{q_e}\right)t \quad (8)$$

where k_2 is the rate constant (g/mg min). The plots of t/q_t versus t give straight lines having slope $1/q_e$ and intercept $1/k_2q^2e$ (Fig. 9). The calculated value of q_e was found to be

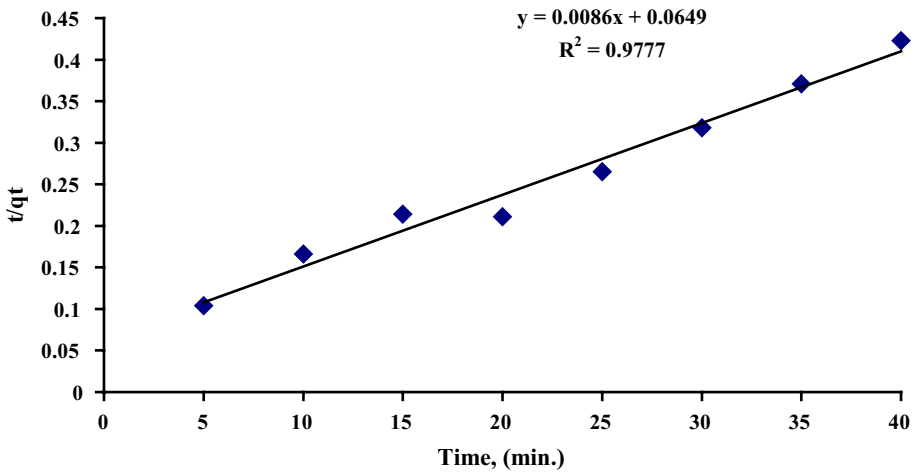

Fig. 9 Pseudo second order model of U(VI) onto the (MOCZ) modified with amine

116.27 mg/g and correlation coefficient (R^2) equal 0.9777 (Table 4).

The obtained data well fitted with the pseudo-second order model. Results were so close to the experimental results (94.5 mg/g). Accordingly, the pseudo-second order model is the most suitable model to describe the kinetics of uranium adsorption by modified MOCZ. This kinetic process is mainly controlled by chemi-sorption, involving chemical bonding between uranyl ions and the adsorbent active sites [70, 71].

Thermodynamic studies of uranium adsorption

Thermodynamics studies focus on the change in energy of the system during adsorption. The change in thermodynamic parameters provides essential information to understand the mechanism of the adsorption process. Thermodynamic parameters are: enthalpy change or the change in heat content (ΔH°, kJ/mol), entropy change (ΔS°, kJ/mol K) and the change in Gibbs free energy (ΔG°, kJ/mol). They are calculated by the following equations [72]:

$$\Delta G = -2.303RT \cdot \mathrm{Log}K_d \quad (9)$$

$$\Delta G = \Delta H - T\Delta S \quad (10)$$

$$\mathrm{Log}K_d = \frac{\Delta S}{2.303R} - \frac{\Delta H}{2.303RT} \quad (11)$$

where K_d is the adsorption equilibrium constant (L/g), R is the universal gas constant (8.314 J/mol K) and T is the absolute temperature (K). By plotting a graph of Log K_d versus 1000/T, K^{-1}, the values ΔH and ΔS were calculated from the slope and intercept (Fig. 10).

The thermodynamic parameters obtained from the plot are listed in (Table 5). The negative values of ΔH° suggest an exothermic adsorption process. The negative values of ΔS° suggest a process involving decrease of randomness. The negative value of ΔG° at room temperature suggests non spontaneous process, while in increasing temperature, positive values of free energy (ΔG°) are encountered; suggesting an unfavored process.

Characterization of MOCZ/amine before and after uranium adsorption

Fourier transform infrared spectrometer characterization

FTIR spectra are useful to identify molecular and functional groups of compounds [73]. Using FTIR model Thermo Scientific Nicolet IS10 instrument, in the range from 400 to 4000 cm^{-1}, the FTIR of zeolite, (MOCZ), (MOCZ) modified with amine before and after adsorption of uranium are given in (Fig. 11A–D). The absorption bands at around 450 cm^{-1} and 1043 cm^{-1} are attributed to Si–O and Si–O–Si of the zeolite framework respectively. The bands contributing to the OH group are observed at 3623 and 3439 cm^{-1}. A band at 1639 cm^{-1} is attributed to the typical deformation band of adsorbed H_2O (Fig. 11A). The broad peak observed between 1400–1500 cm^{-1} and the small peak at 875 cm^{-1} in the MnO_2/zeolite sample may be attributed to the presence of MnO_2 (Fig. 11B).

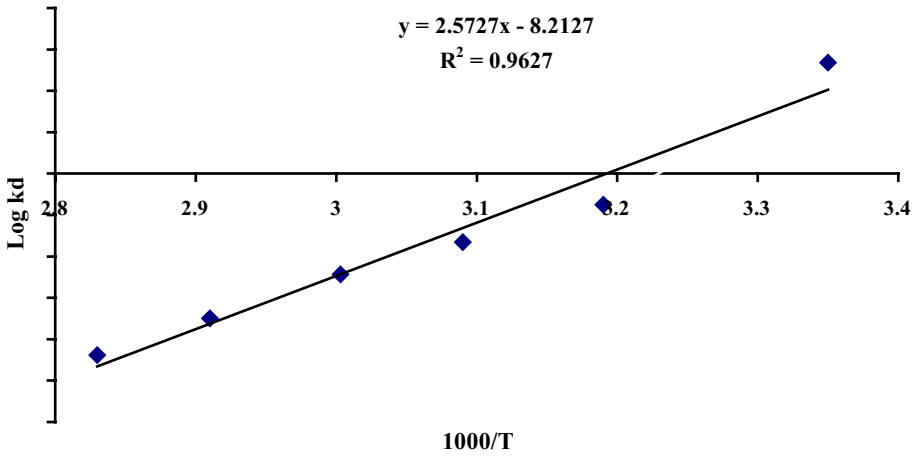

Fig. 10 log K_d versus 1000/T for uranium adsorption onto (MOCZ) modified with amine

Table 5 Thermodynamic parameters for U(VI) adsorption by MOCZ modified with amine

Adsorbent	ΔH (kJ/mol)	ΔS (kJ/mol K^{-1})	ΔG (kJ/mol)					
MOCZ/ amine	− 49.25	− 0.1550	298 °K	313 °K	323 °K	333 °K	343 °K	353 °K
			− 3.05	0.89	2.05	3.10	4.59	5.92

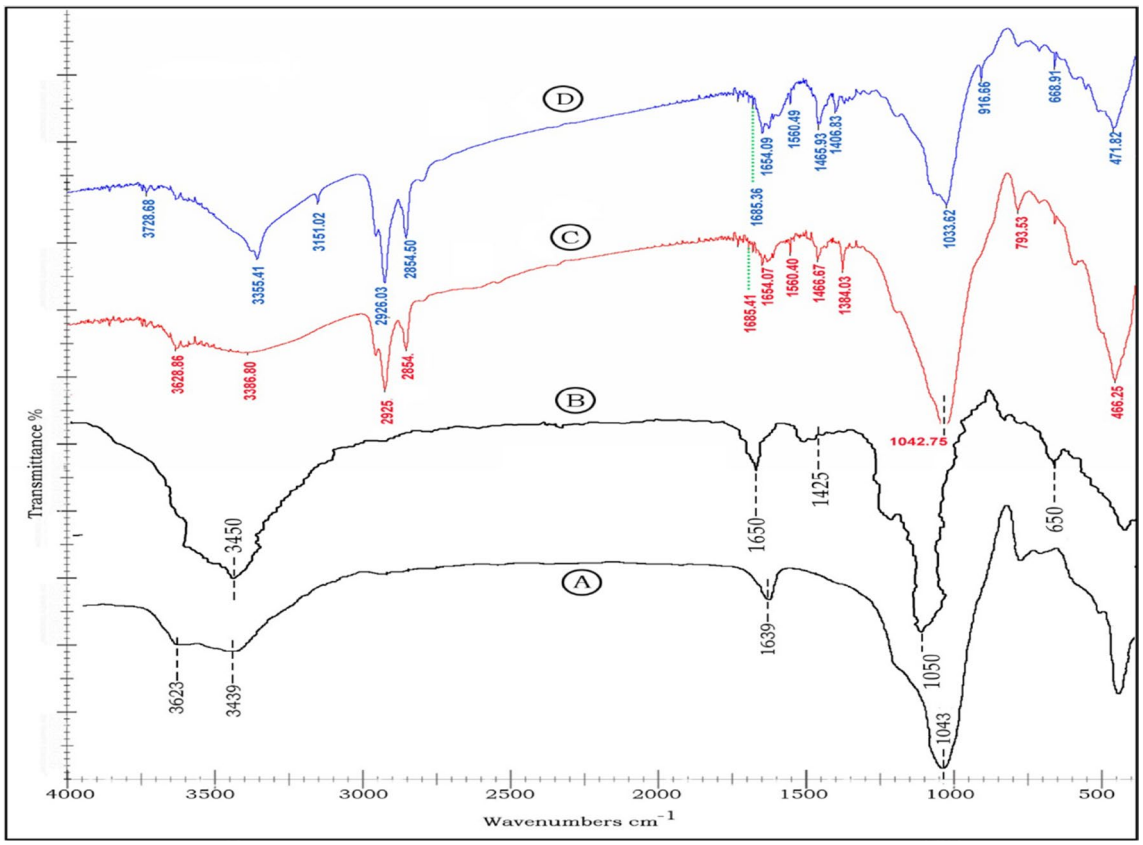

Fig. 11 FTIR chart of the zeolite (A), (MOCZ) (B), (MOCZ) modified with amine (C) and (MOCZ) after adsorption of uranium (D)

MOCZ/amine showed a peak at 3728.68 cm^{-1} that corresponds to –OH free stretching. The peak at 3355.41 cm^{-1} corresponds to N–H stretch. The band at 3151.02 cm^{-1} is due to Ar–H stretching and [=CH stretching, (m, s)]. The peaks at 2926.03 and 2854.50 cm^{-1} correspond to CH_2 stretching (m,s). The two bands at 1685.36 and 1654.09 cm^{-1} are related C=O stretching. The peak at 1560.49 cm^{-1} corresponds to out of plane N–H bending. The strong band at 1465.93 cm^{-1} appeared due to CH_2 and CH_3 (s).

The band at 1406.83 is related to aromatic C–C stretching. While, the band at 1033.62 cm^{-1} is corresponds to C–N stretching (m). The peak at 916.66 cm^{-1} corresponds to =CH out of plane bending. The bands at 668.91 and 471.82 cm^{-1} are related to C=C aromatic out of plane bending (Fig. 11C). The peak at 3151.02 cm^{-1} disappeared after adsorption of uranium, while the peak at 793.53 cm^{-1} appeared. Most bands are shifted, indicating adsorption of uranium (Fig. 11D).

Scanning electron microscope (SEM)

Natural zeolite sample from Yemeni origin, supplied by Alix Zeolite Co., Egypt, was scanned by SEM. The main existing mineral is clinoptilolite with Si/Al ratio of 5.0. Natural zeolite shows a highly active surface area with high sorption ability, which makes it an effective sorbent for use (Fig. 12A).

Clear MnO_2 particles persist on the surface of zeolite crystals. It was shown recently that upon coating zeolite with MnO_2, the specific surface area increase due to the creation of MnO_2 structures [74] (Fig. 12B). The Scanning electron microscope image (Fig. 12C) showed that the surface of zeolite was coated completely with manganese oxide and modified with amine. On the other hand, the image of the surface after adsorption of uranium is shown in (Fig. 12D). EDX spectra of the studied modified MOCZ before and after uranium adsorption is shown in (Fig. 12E, F) indicating that uranium was successfully adsorbed. The main component of MOCZ/ amine before adsorption of uranium are Mn (50.2%), Si (40.8%), Al (4.5%), K (4.5%), (Fig. 12E). While, the component of MOCZ/ amine after adsorption of uranium are Si (40.6%), Mn (35.4%), K (8.4%), Al (5.2%), U (10.4%), (Fig. 12F).

Case study

Obtained Hammamat sedimentary sample from Gattar area with uranium concentration 2400 mg/Kg was ground to particle size –200 mesh and subjected to acid leaching at the

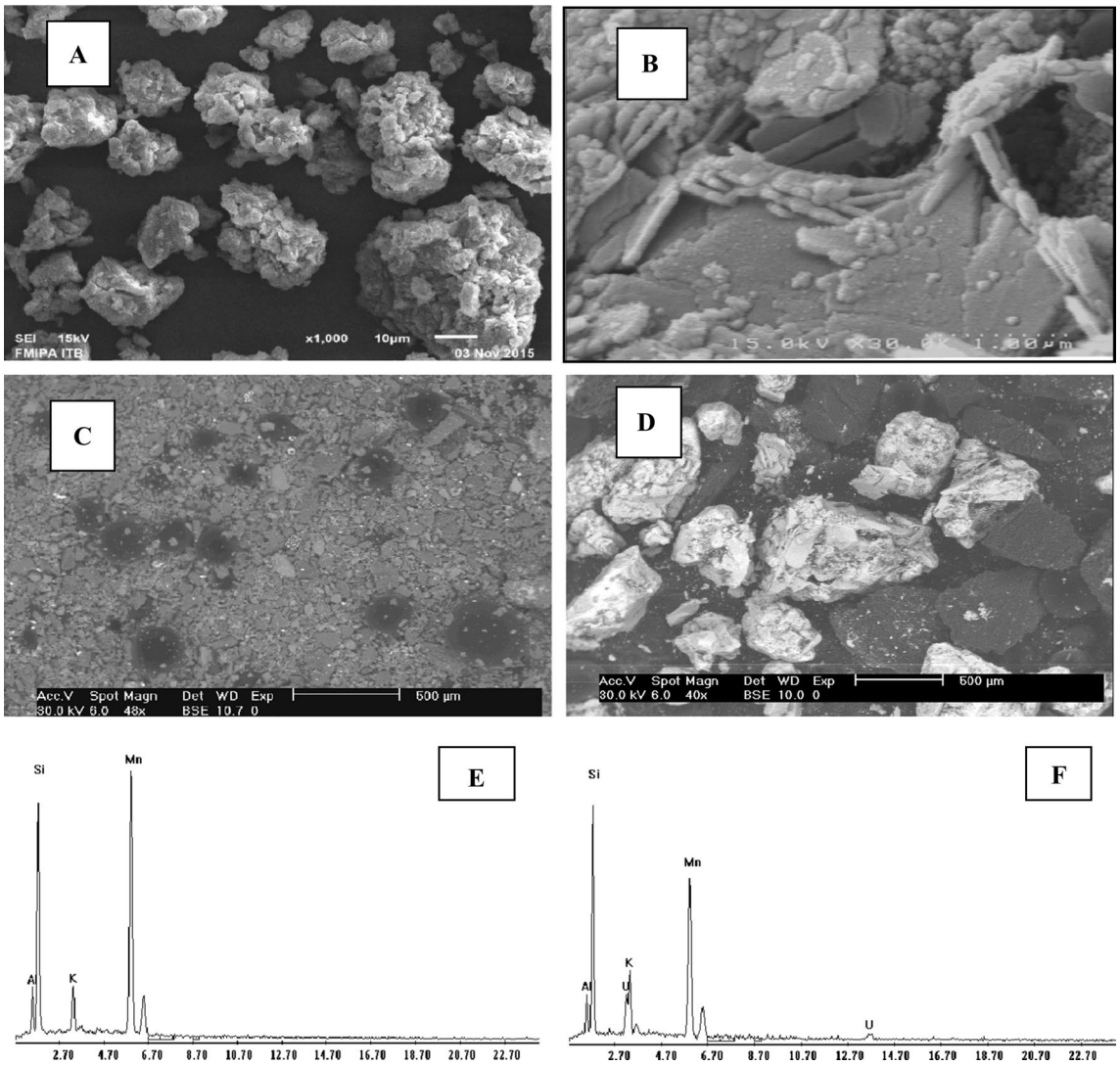

Fig. 12 SEM of the Natural Zeolite (**A**), (MOCZ) (**B**), (MOCZ) modified with amine (**C**) and (MOCZ) with amine after adsorption of uranium (**D**), EDX of (MOCZ) modified with amine before (**E**) and after U(VI) adsorption (**F**)

following conditions: 5.0 M H_2SO_4 acid with ratio 1:4 (S/L) for 30 min at room temperature. Leaching efficiency reached 85%. The resulting leach liquor was filtered and uranium was estimated as 510 mg/L. 4 L of the filtered leach liquor were mixed with 5.1 g of the (MOCZ) modified with amine at the optimum conditions (pH 4, 200 rpm stirring speed, 20 min contact time at room temperature). Uranium(VI) was eluted from the loaded modified (MOCZ) using 0.3 M H_2SO_4 acid and was precipitated using sodium hydroxide at pH 7 as sodium diuranate ($Na_2U_2O_7$), then dried at 110 °C for 1 h. The final precipitate was identified by ICP-OES to determine uranium content and its impurities (Table 6). Uranium content assayed 68% attaining a purity of 90.66% with decreased content of metal ion impurities. A comparative study for uptake capacity (mg/g) of different adsorbents toward uranium is shown in (Table 7).

Conclusion

MOCZ modified with amine was used efficiently for uranium adsorption. The optimum adsorption conditions were found to be at pH 4, 200 rpm stirring speed, 20 min contact time, 0.1 g of modified MOCZ/ amine and 20 mL of uranium solution containing 500 mg/L at room temperature. The maximum uptake capacity reached 99 mg/g. The studied process kinetics fitted well with pseudo-second order kinetic model. The adsorption mechanism was explained according to Langmuir adsorption isotherm model assumptions. Uranium desorption using 0.3 M H_2SO_4. Optimum conditions were carried out for uranium recovery from Hammamat sediment of Gattar area, North Eastern Desert, Egypt. The final uranium precipitate was characterized by ICP-OES technique.

Table 6 ICP-OES specification of uranium concentrate produced by (MOCZ) / amine

Element	U	Si	Al	P	Ca	Mg	Co	Ni	Cu
Content (%)	68.00	0.0069	0.0090	0.0010	0.0690	0.0490	0.0002	0.0010	0.0030
Element	Ba	Cr	Na	K	Mn	Ti	Zn	Pb	Zr
Content (%)	0.0019	0.0021	6.5170	0.0101	0.0090	0.0080	0.0019	0.0020	0.0015

Table 7 The comparison of uranium adsorption capacity by different adsorbents

Adsorbent	Conditions	Q_{max} mg/g	Ref.
Natural zeolite	pH = 3.0, T = 298 K	8.70	[10]
MOCZ	pH = 4.0, T = 293 K	15.1	[11]
P(HEMA-EP)	pH = 4.0, T = 298 K	104.72	[3]
MOCZ	pH = 5.0, T = 298 K	18.1	[43]
P1 zeolites	pH = 2.5, T = 293 K	3.72	[12]
Ambersep 920U SO_4	pH = 2, T = 298 K	58	[25]
Polypyrrole	pH = 5, T = 298 K	87.72	[75]
Olive stones activated with $ZnCl_2$	pH = 6, T = 298 K	57.80	[76]
β-cyclodextrin magnetic bentonite nano composite	pH = 5, T = 298 K	305	[77]
Chitosan	pH = 3, T = 298 K	72.46	[78]
Banyan leaves	pH = 3, T = 298 K	33.44	[79]
Anionic resin Dowex A	pH = 3.9, T = 298 K	79	[80]
Tea waste	pH = 4, T = 298 K	29.41	[81]
Modified (MOCZ/amine)	pH = 4, T = 298 K	99	Present study

Funding This work was funded by the Nuclear Materials Authority as a part of its research activities. This article was reviewed and approved for publishing by the Nuclear Materials Authority with no obligation on the authors' part to revise the manuscript.

Compliance with ethical standards

Conflict of interest The authors declare that they have no conflict of interest.

References

1. Ozay O, Ekici S, Aktas N, Sahiner N (2011) J Environ Manag 92:3121. https://doi.org/10.1016/j.jenvman.2011.08.004
2. Attallah MF, Hassan HS, Youssef MA (2019) J Appl Radiat Isotop 147:40. https://doi.org/10.1016/j.apradiso.2019.01.015
3. Akkaya R, Akkaya B (2013) J Nucl Mater 434:328. https://doi.org/10.1016/j.jnucmat.2012.11.056
4. Shapkin NP, Ermak IM, Razov VI (2014) Russ J Inorg Chem 59:587. https://doi.org/10.1134/S0036023614060187
5. Choi H, Yu SW, Kim KH (2016) J Taiw Inst Chem Eng 63:482. https://doi.org/10.1016/j.jtice.2016.03.005
6. Yamaguchi N, Taniyama I, Kimura T, Yoshioka K, Saito M (2016) Soil Sci Plant Nutr 62(3):303. https://doi.org/10.1080/00380768.2016.1196119
7. Ramesh K, Reddy DD (2011) Adv Agron 113:219. https://doi.org/10.1016/B978-0-12-386473-4.00004-X
8. Shapkin NP, Shkuratov AL, Razov VI (2014) Russ J Inorg Chem 59:1004. https://doi.org/10.1134/S0036023614090150
9. Misaelides P, Godelitsas A, Filippidis A, Charistos D, Anousis I (1995) Sci Total Environ 173:237. https://doi.org/10.1016/0048-9697(95)04748-4
10. Han R, Zou W, Wang Y, Zhu L (2007) J Environ Radiol 93:127. https://doi.org/10.1016/j.jenvrad.2006.12.003
11. Barkat M, Nibou D, Amokrane S, Chegrouche S, Mellah A (2015) C R Chim 18:261. https://doi.org/10.1016/j.crci.2014.09.011
12. Nouh E, Amin M, Gouda M, Abd-Elmagid A (2015) J Environ Chem Eng 3:523. https://doi.org/10.1016/j.jece.2015.01.013
13. Shamsan SO, Gaikwad DK, Sayyed MI, Al-Rashdi K, Pawar PP (2018) Mat Today Proc 5:17930. https://doi.org/10.1016/j.matpr.2018.06.122
14. Cinar S, Baykal BB (2005) Water Sci Technol 51(11):71. https://doi.org/10.2166/wst.2005.0392
15. Blatov VA, Ilyushin GD, Proserpio DM (2010) J Inorg Chem 49(4):1811. https://doi.org/10.1021/ic9021933
16. Tsitsishvili V, Dolaberidze N, Urotadze S, Alelishvili M, Mirdzveli N, Nijaradze M (2017) Chem J Moldova 12(1):95. https://doi.org/10.19261/cjm.2017.413
17. Sharma P, Han MH, Cho CH (2015) J Nanomater 1:1. https://doi.org/10.1155/2015/912575
18. Rhodes CJ (2010) Sci Prog 93(3):223. https://doi.org/10.3184/003685010X12800828155007
19. Zou W, Zhang J, Li K, Han P, Han R (2009) Adsorp Sci Technol 27(6):549. https://doi.org/10.1260/0263-6174.27.6.549
20. Lyu C, Yang X, Zhang S, Zhang Q, Su X (2017) Environ Technol 40:1. https://doi.org/10.1080/09593330.2017.1410579
21. Krivoshapkin P, Ivanets A, Torlopov M, Mikhaylov V, Srivastava V, Sillanpää M, Prozorovich VG, Kuznetsova T, Koshevaya E,

Krivoshapkina E (2019) Carbohydr Polym 210:135. https://doi.org/10.1016/j.carbpol.2019.01.045
22. Zemskova LA, Voit AV, Barinov NN (2016) Russ J Inorg Chem 61:1567. https://doi.org/10.1134/S0036023616120226
23. Babel S, Kurniawan TA (2003) J Hazard Mater 97(3):219. https://doi.org/10.1016/S0304-3894(02)00263-7
24. Sayyah EM, El-hussaini OM, Abd El-Ghany MS, Abuzaid AHM, Abd-El Gawad HH (2012) Arab J Nucl Sci Appl 45:130
25. Cheira MF, Atia BM, Kouraim MN (2017) J Radiat Res Appl Sci 10:307. https://doi.org/10.1016/j.jrras.2017.07.005
26. Han Q, Du M, Guan Y, Luo G, Zhang Z, Li T, Ji Y (2020) Chem Phys Lett. https://doi.org/10.1016/j.cplett.2020.137092
27. Datta D, Uslu H, Kumar S (2015) J Chem Eng 60(11):3193. https://doi.org/10.1021/acs.jced.5b00413
28. Pourreza N, Parham H, Pourbati MA (2015) Desalin Water Treat 57(37):1. https://doi.org/10.1080/19443994.2015.1086892
29. Lashaki MJ, Khiavi S, Sayari A (2019) Chem Soc Rev 48(12):3320. https://doi.org/10.1039/C8CS00877A
30. Lamy-Mendes A, Torres RB, Vareda JP, Lopes D, Ferreira M, Valente V, Girão AV, Valente AJM, Durães L (2019) Molecules 24(20):3701. https://doi.org/10.3390/molecules24203701
31. Faghihian H, Nourmoradi H, Shokouhi M (2012) Pol J Chem Technol 14:50. https://doi.org/10.2478/v10026-012-0059-4
32. Faghihian H, Nourmoradi H, Shokouhi M (2013) Desalin Water Treat 52:305. https://doi.org/10.1080/19443994.2013.785367
33. Ali Z, Khan A, Ahmad R (2015) Microporous Mesoporous Mater 203:8. https://doi.org/10.1016/j.micromeso.2014.10.004
34. Xiaonan D, Genggeng Q, Peng W, Giannelis EP (2012) Chem Phys Chem 13:2536. https://doi.org/10.3390/molecules24203701
35. Vareda JP, Durães L (2017) J Sol Gel Sci Technol 84:400. https://doi.org/10.1007/s10971-017-4326-y
36. Vareda JP, Durães L (2019) Environ Technol 40:529. https://doi.org/10.1080/09593330.2017.1397766
37. Vareda JP, Valente AJM, Durães L (2019) J Environ Manag 246:101. https://doi.org/10.1016/j.jenvman.2019.05.126
38. Mathew KJ, Mason B, Morales ME, Narayann UI (2009) J Radioanal Nucl Chem 282:939. https://doi.org/10.1007/s10967-009-0186-4
39. Marczenko Z, Balcerzak M (2000) Uranium. In: Separation, preconcentration and spectrophotometry in inorganic analysis, vol 10. Elsevier, pp 446–455. https://doi.org/10.1016/S0926-4345(00)80118-2
40. Shapiro L, Brannock WW (1962) US Geological Survey Bulletin (Revised Edition), vol 114A. United States Government Printing Office, Washington
41. Govindaraju K, Mevelle C, Chouard C (1976) Anal Chem 48:1325
42. Runping H, Weihua Z, Wang Y (2007) J Environ Radioactiv 93(3):127. https://doi.org/10.1016/j.jenvrad.2006.12.003
43. Weihua Z, Lei Z, Runping H (2009) Chin J Chem Eng 17(4):585. https://doi.org/10.1016/S1004-9541(08)60248-7
44. Ferrah N, Abderrahim O, Didi MA, Villemin D (2011) J Radioanal Nucl Chem 289:721. https://doi.org/10.1007/s10967-011-1172-1
45. Wan Ngah WS, Endud CS, Mayanar R (2002) React Funct Polym 50(2):181. https://doi.org/10.1016/S1381-5148(01)00113-4
46. Tsezos M, Volesky B (1982) Biotechnol Bioeng 24:385
47. Yahia M, Torkia Y, Knani S, Hachicha MA, Khalfaoui M, Ben Lamine A (2013) Ads Sci Technol 31:341. https://doi.org/10.1260/0263-6174.31.4.341
48. Mishra SP, Ganga P, Raju A, Mira D (2012) J Chem Pharma Res 4(2):1207
49. Panda H, Tiadi N, Mohanty M, Mohanty CR (2017) S Afr J Chem Eng 23:132. https://doi.org/10.1016/j.sajce.2017.05.002
50. Firas SA (2013) Adv Natur Appl Sci 7(3):336
51. Miraoui A, Didi MA (2015) Eur Chem Bull 4(11):512. https://doi.org/10.17628/ECB.2015.4.512
52. Nyquist RA, Craver CD (1977) In: Craver CD (ed) The coblentz society desk book of infrared spectra. The Coblentz Society, French Village (MO), p 399p
53. Yousef LA, Morsy AMA, Hagag MS (2020) Sep Sci Technol 55(4):648. https://doi.org/10.1080/01496395.2019.1574305
54. Morsy AMA (2015) Environ Technol Innov 4:299. https://doi.org/10.1016/j.eti.2015.10.002
55. Yousef LA, Bakry AR, Abd El Magied MO (2019) J Radioanal Nuclear Chem. https://doi.org/10.1007/s10967-019-06871-5
56. Yousef LA, Bakry AR, Ahmad AA (2019) SN Appl Sci 1:974. https://doi.org/10.1007/s42452-019-1006-2
57. Das DP, Das J, Parida K (2003) Colloid Interface Sci 261:213. https://doi.org/10.1016/S0021-9797(03)00082-1
58. Liao XP, Shi B (2005) Environ Sci Technol 39:4628. https://doi.org/10.1021/es0479944
59. Chaudhary N, Balomajumder C (2014) Taiwan Inst Chem Eng 45:852. https://doi.org/10.1016/j.jtice.2013.08.016
60. Kannamba B, Reddy KL, Apparao BV (2010) Hazard Mater 175:935. https://doi.org/10.1016/j.jhazmat.2009.10.098
61. Wen Z, Niu Y (2017) IOP Conf Ser Mater Sci Eng 191:012035. https://doi.org/10.1088/1757-899X/191/1/012035
62. Chabani M, Amrane A, Bensmaili A (2006) J Chem Eng 125:111. https://doi.org/10.1016/j.cej.2006.08.014
63. Weber TW, Chakraborti RK (1974) Am Inst Chem Eng 20:228. https://doi.org/10.1166/asem.2015.1664
64. Langmuir I (1918) Am Chem Soc 40:1361. https://doi.org/10.1021/ja02242a004
65. Tunali S, Akar T (2006) Hazard Mater 131:137. https://doi.org/10.1016/j.jhazmat.2005.09.024
66. Humelnicu D, Drochioiu G, Sturza MI, Cecal A, Popa K (2006) Radioanal Nucl Chem 270:637. https://doi.org/10.1007/s10967-006-0473-2
67. Freundlich HMF (1906) Phys Chem 57:385
68. Lagergren S (1898) Kungliga Svenska Vetenskapsakademiens Handlinger 24:1
69. Zhang X, Jiao C, Wang J, Liu Q, Li R, Yang P (2012) Chem Eng 198:412. https://doi.org/10.1016/j.cej.2012.05.090
70. Wu FC, Tseng RL, Juang RS (2001) J Hazard Mater 81:167. https://doi.org/10.1016/S0304-3894(00)00340-X
71. Ding L, Deng HP, Wu C, Han X (2012) Chem Eng 181:360. https://doi.org/10.1016/j.cej.2011.11.096
72. Bayramoglu G, Arica MY (2011) Water Air Soil Poll 221:391. https://doi.org/10.1007/s11270-011-0798-5
73. Dong J, Ozaki Y (1997) Macromolecules 30:286. https://doi.org/10.1021/ma9607168
74. Azar PR, Falamaki C (2012) J Ind Eng Chem 18:737. https://doi.org/10.1016/j.jiec.2011.11.112
75. Abdi S, Nasiri M, Mesbahi A, Khani MH (2017) J Hazard Mater 332:132. https://doi.org/10.1016/j.jhazmat.2017.01.013
76. Kütahyal C, Eral M (2010) J Nucl Mater 396(2):251. https://doi.org/10.1016/j.jnucmat.2009.11.018
77. Zahran F, El-Maghrabi HH, Hussein G, Abdelmaged SM (2019) Environ Nanotechnol Monit Manag 11:100205. https://doi.org/10.1016/j.enmm.2018.100205
78. Wang G, Liu J, Wang X, Xie Z, Deng N (2009) J Hazard Mater 168(2):1053. https://doi.org/10.1016/j.jhazmat.2009.02.157
79. Xia LK, Wang X, Zheng W (2013) J Environ Eng 139(6):887. https://doi.org/10.1061/(ASCE)EE.1943-7870.0000695
80. Claudia A, Ladeira Q, Renato C, Alves G (2007) J Hazard Mater 148(3):499. https://doi.org/10.1016/j.jhazmat.2007.03.003
81. Li X, Li F, Jin Y, Jiang C (2015) J Mol Liq 209:413. https://doi.org/10.1016/j.molliq.2015.06.014